Inhibiting the Formation of Neutrophil Extracellular Traps to Prevent the Recurrence of Post-operative Glioblastoma

Yaobao Han[1], Mengxiao Han[1], Tingting Wang[1], Hao Zhang[1], Hanghang Liu[1, 2], Yanhui Zheng[1], Jun Dong[3], Zhen Li[1, *]

[1] State Key Laboratory of Radiation Medicine and Protection, School of Radiation Medicine and Protection, Collaborative Innovation Center of Radiation Medicine of Jiangsu Higher Education Institutions, Soochow University, Suzhou 215123, China

[2] Hubei Key Laboratory of Natural Products Research and Development and College of Biological and Pharmaceutical Science, China Three Gorges University, Yichang 443002, China

[3] Department of Neurosurgery, Second Affiliated Hospital of Soochow University, Suzhou, China

Email: zhenli@suda.edu.cn

Table S1. The atomic ratio of Cu and Se in CS nanozyme determined by inductively coupled plasma-optical emission spectrometry (ICP–OES) and X-ray photoelectron spectroscopy (XPS), respectively.

Element at%	In precusor	In product by ICP-OES	In product by XPS
Cu	100%	36.18%	33.69%
Se	200%	63.82%	66.31%

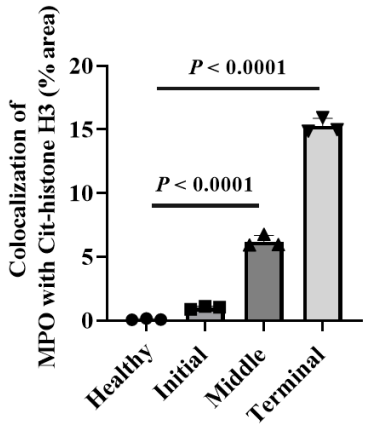

Figure S1. Quantitative analysis of the colocalization of MPO with Cit-histone H3 (% area) in different stages of GBM by ImageJ. n = 3 independent experiments per group. The data were presented as the means ± s.d. One-way ANOVA with Tukey's post hoc test was used for comparisons among multiple groups. Source data were provided as a Source Data file.

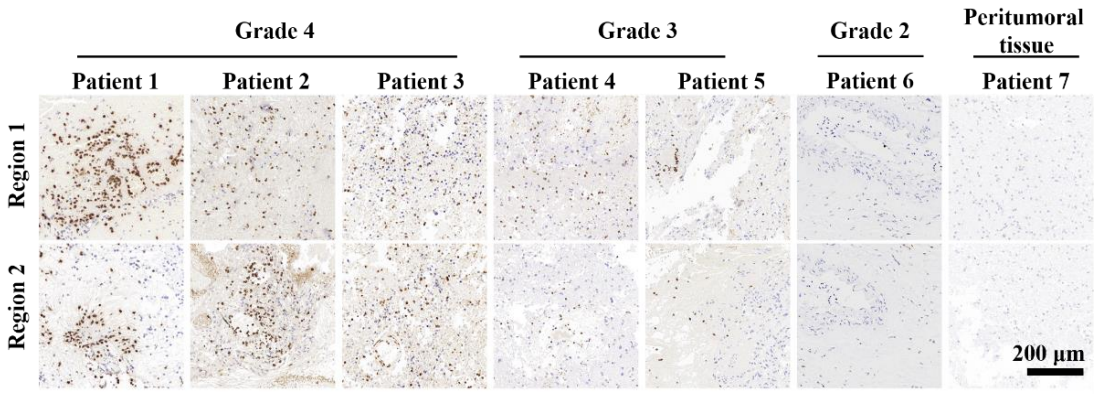

Figure S2. More immunohistochemical staining regions showed neutrophils infiltrating into different grades of glioma tissues. Areas chosen for analysis were absence or sparce of blood cells to avoid confounding effects during microscopic examination.

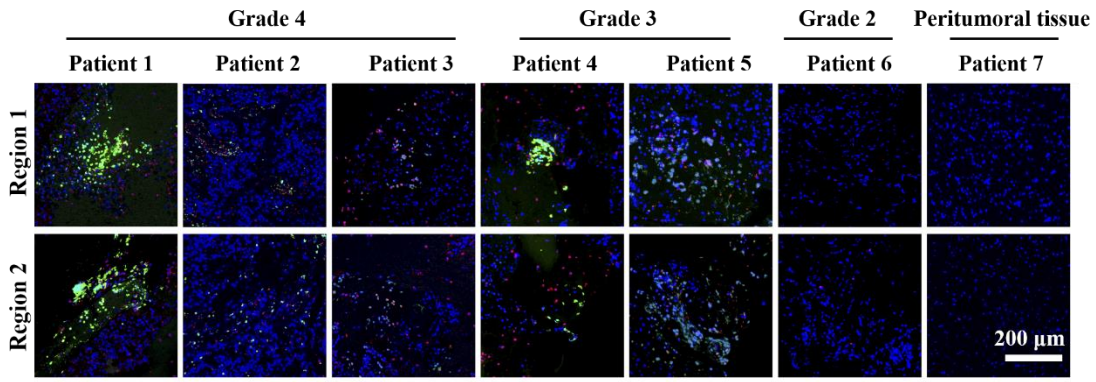

Figure S3. More immunofluorescence staining regions showed NETs infiltrating into different grades of glioma tissues. NETs were identified by the colocalization of myeloperoxidase (MPO, red) and citrullinated histone H3 (Cit-histone H3, green). NETs were abundant in both grade 4 and 3 glioma tissues, but only a few in grade 2 glioma tissues, and none in peritumoral tissue. Areas chosen for analysis were absence or sparce of blood cells to avoid confounding effects during microscopic examination.

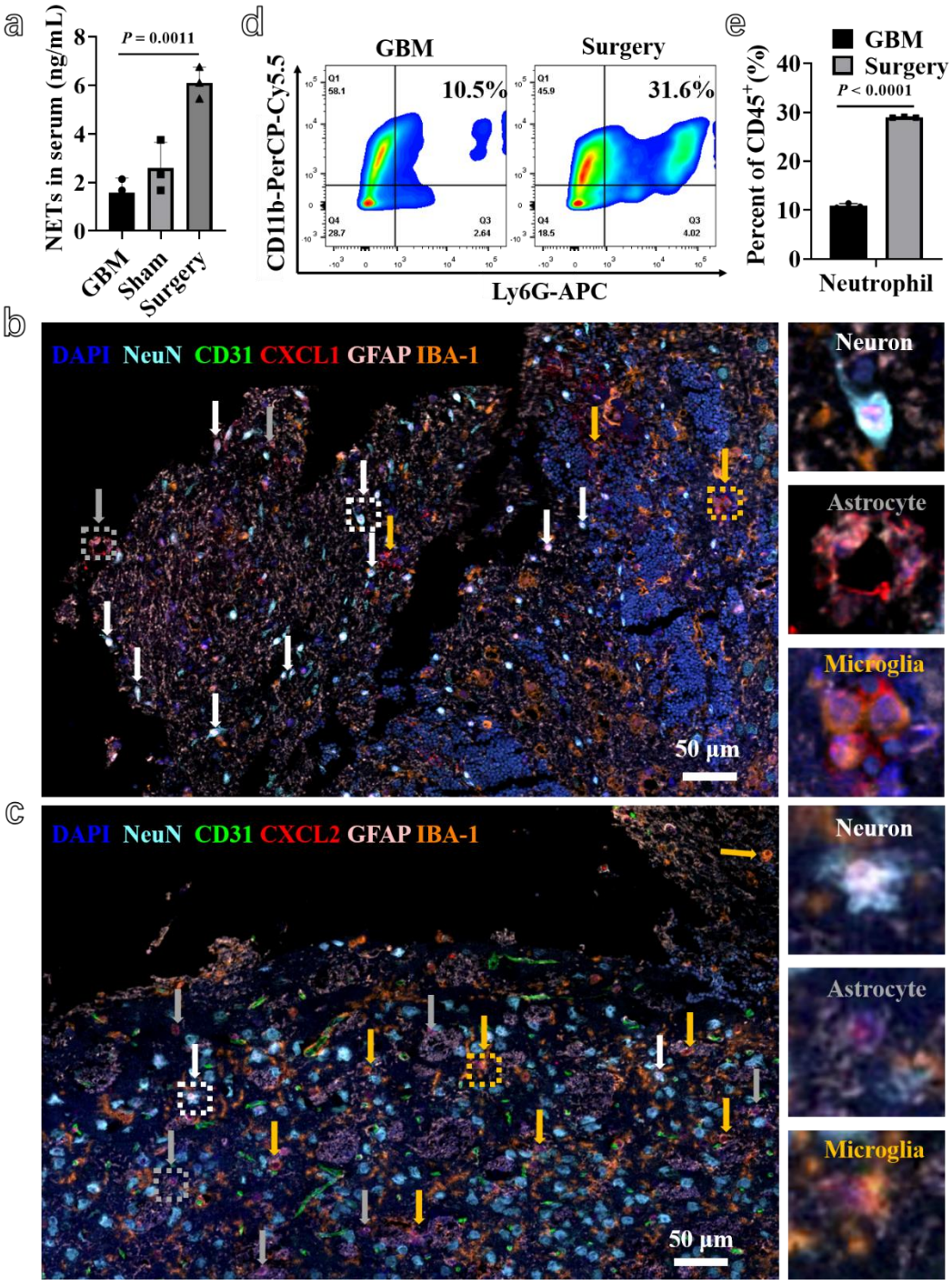

Figure S4. (a) NETs concentration in the blood serum of mice from different groups as determined by ELISA kits. The brain of tumor-bearing mice without surgery was selected as the GBM group, the brain with partially resected tumor was selected as the sham group and the brain with fully resected tumor was selected as the surgery group. n = 3 independent experiments per group. (b) Expression of CXCL1 in brain tissue after the surgery of GBM. Nuclei (DAPI, blue). Neurons (NeuN, cyan). Vascular endothelial

cells (CD31, green). CXCL1, red. Astrocytes (GFAP, pink). Microglia (IBA-1, orange). The expression of CXCL1 by neurons (NeuN) was indicated by white arrows. The expression of CXCL1 by astrocytes (GFAP) was denoted by gray arrows. The expression of CXCL1 by microglia (IBA-1) was marked by golden arrows. (c) CXCL2 expression profile showing similar cellular localization pattern to CXCL1. (d-e) Neutrophils ratio of $CD45^+$ in GBM and the surgery site postoperative glioblastoma assayed by flow cytometry. n = 3 independent experiments per group. The data were presented as the means ± s.d. One-way ANOVA with Tukey's post hoc test was used for comparisons among multiple groups (a) and a two-sided Student's t test was used for comparison between two groups (e). Source data were provided as a Source Data file.

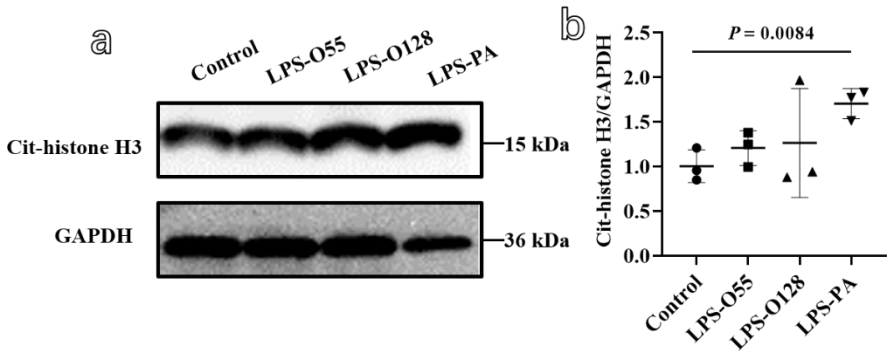

Figure S5. Formation of NETs in the neutrophils treated with different types of LPS. (a) Western blot analysis of Cit-histone H3 in different groups of neutrophils. (b) The quantitative analysis of Western blot of Cit-histone H3 in different groups of neutrophils. Neutrophils were treated with 10 μg/mL different types of LPS purchased from Sigma-Aldrich. n = 3 independent experiments per group. The data were presented as the means ± s.d. Two-sided Student's t test was used for comparison between Control and LPS-PA groups. (b). Source data were provided as a Source Data file.

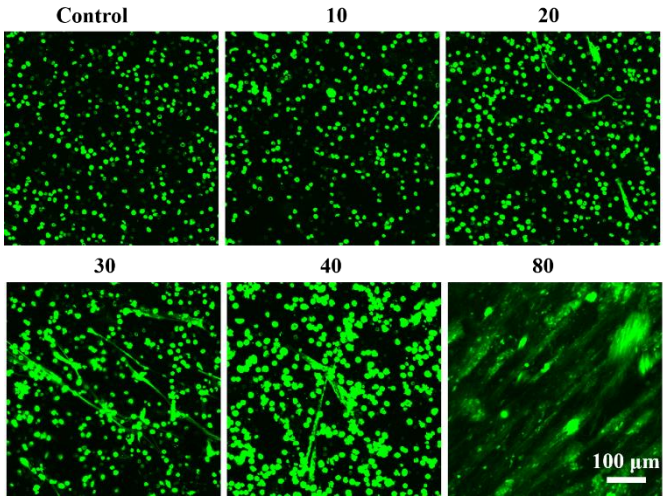

Figure S6. CLSM images of nuclear decondensation in different groups of neutrophils stained by SYTOX Green. Neutrophils were treated with different concentrations of LPS-PA (0, 10, 20, 30, 40, 80 μg/mL) for 3 h. n = 3 independent experiments per group.

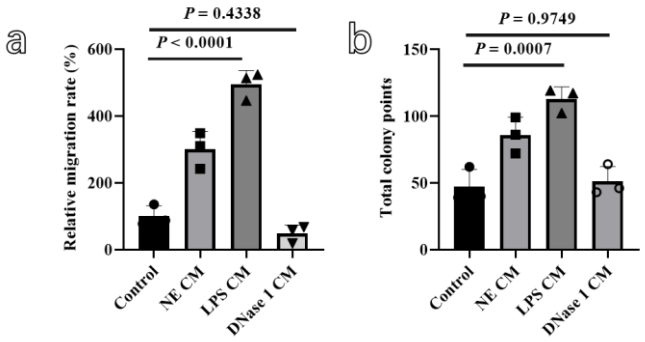

Figure S7. (a) Relative migration rate of GL261 cells after different treatments. (b) Clone formation assay of GL261 cells stained by crystal violet in different groups. GL261 cells were treated with medium contain 1% FBS (control), neutrophils medium (NE CM), medium collected from neutrophils treated with LPS (LPS CM) or medium collected from neutrophils treated with LPS and DNase 1 (DNase 1 CM). n = 3 independent experiments per group. The data were presented as the means ± s.d. One-way ANOVA with Tukey's post hoc test was used for comparisons among multiple groups (a and b). Source data were provided as a Source Data file.

Figure S8. The hydrogelation ability of Matrigel before and after being heated at 37 ℃ for 10 min.

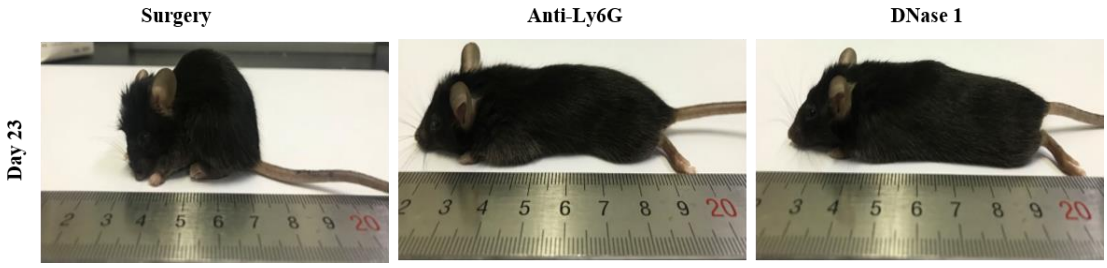

Figure S9. Representative photographs of mice from the surgery group, anti-Ly6G antibody treated group, and DNase 1 treated group taken at 23 days after inoculation of tumor cells.

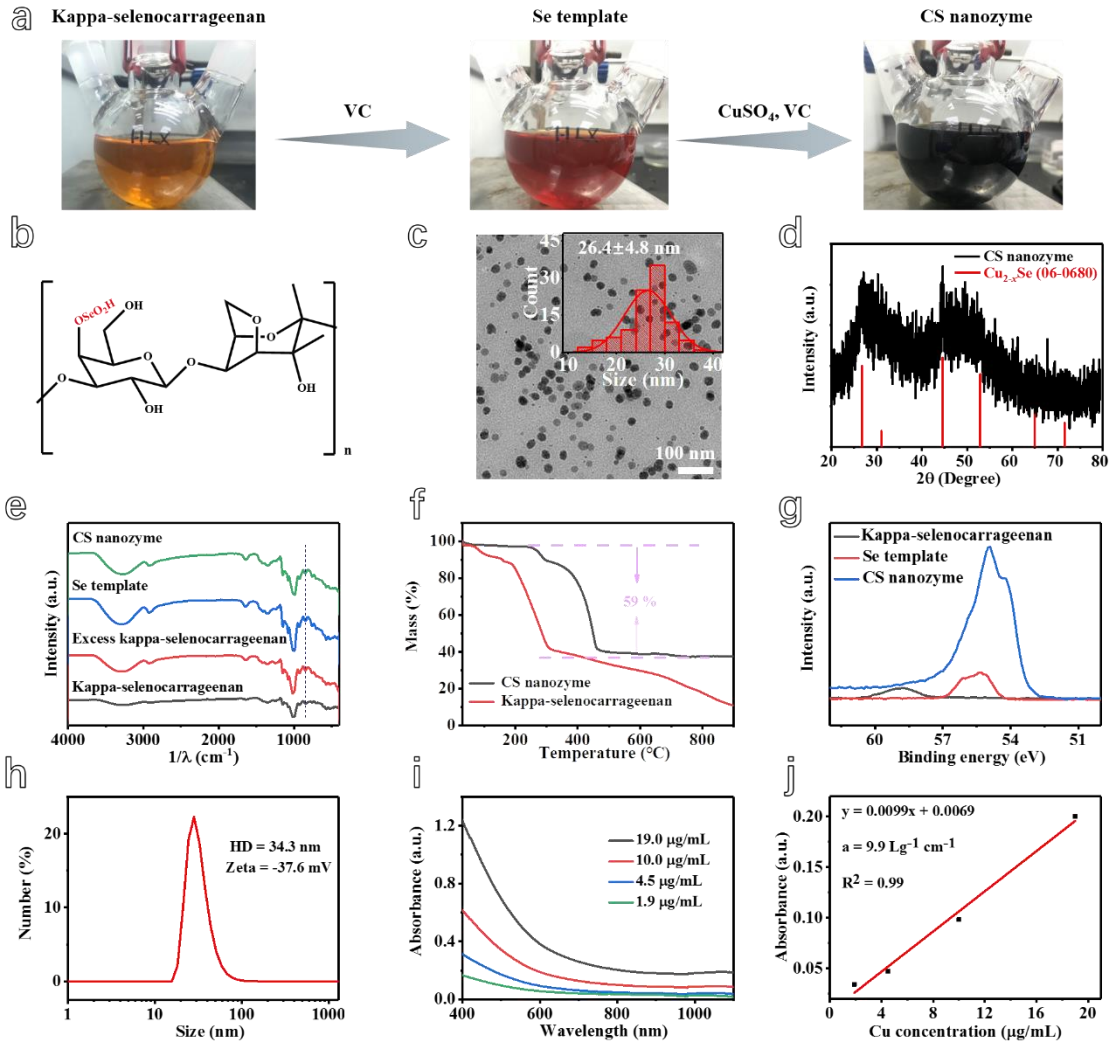

Figure S10. Characterization of as prepared CS nanozyme. (a) The preparation process of CS nanozyme. (b) Structural formula of kappa-selenocarrageenan. (c) TEM image (insert: size distribution of CS nanozyme counted from TEM image). (d) XRD patterns of CS nanozyme. (e) Fourier-transform infrared spectroscopy (FTIR) spectra of kappa-selenocarrageenan, excess kappa-selenocarrageenan, Se template, and CS nanozyme. (f) Thermal gravimetric analysis (TGA) curves of CS nanozyme and kappa-selenocarrageenan. (g) XPS spectra of selenium element in kappa-selenocarrageenan-derived Se template and CS nanozyme. (h) Hydrodynamic size of CS nanozyme. (i) The UV–Vis–NIR spectra of CS nanozyme solution with different concentrations. (j) Concentration dependent absorbance of CS nanozyme at 808 nm. Source data were provided as a Source Data file.

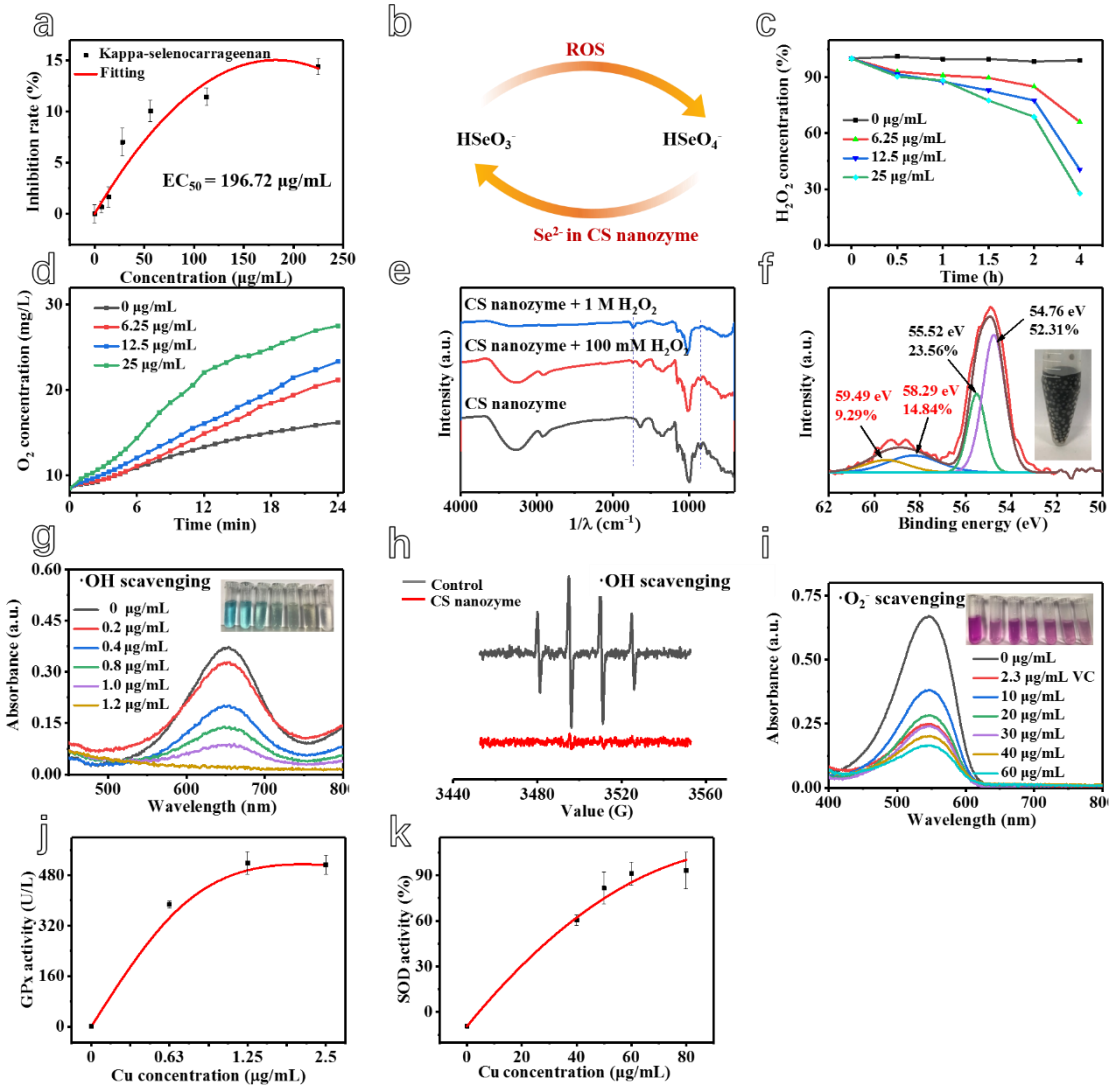

Figure S11. Assessment of the excellent multienzyme-like activities of CS nanozyme. (a) Free radical scavenging rate of kappa-selenocarrageenan. (b) The synergistic mechanism between kappa-selenocarrageenan and the CS nanozyme to scavenge ROS. (c–d) The concentration-dependent degradation of H_2O_2 and generation of O_2. H_2O_2 concentration was detected through the $Ti(SO_4)_2$ method. O_2 concentration was measured by a dissolved oxygen meter. (e) FTIR spectra of CS nanozyme before and after reaction with different concentrations of H_2O_2. (f) XPS spectra of CS nanozyme after reaction with 1 M H_2O_2 (insert: photograph of the bubble formatted during the reaction). (g–h) Ability of CS nanozyme scavenging ·OH radicals assayed by UV–Vis–NIR spectra (insert: photograph of different solutions) and ESR. (i) Ability of CS nanozyme scavenging $\cdot O_2^-$ radicals assayed by UV–Vis–NIR spectra (insert:

photograph of different solutions). (j–k) Assay of concentration-dependent multienzyme-like activities of CS nanozyme, *i.e.* GPx-like activity, and SOD-like activity. n = 3 independent experiments per group. Source data were provided as a Source Data file.

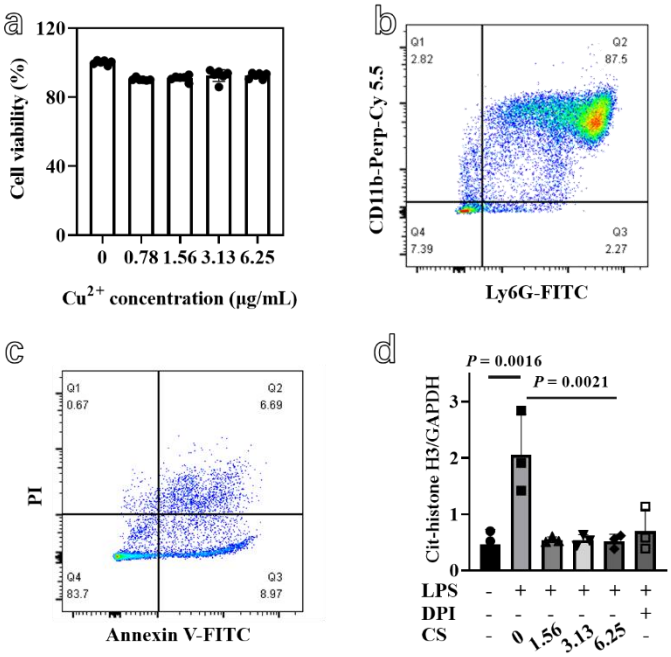

Figure S12. (a) Cytotoxicity of CS nanozyme toward neutrophils assayed by CCK-8 method. n = 6 independent experiments per group. (b) Flow cytometric analysis of the purity of neutrophils collected from the bone marrow of mice, determined by using CD11b-Percp-Cy5.5 and Ly6G-FITC antibodies. (c) Flow cytometric analysis of the activity of collected neutrophils by using annexin V-FITC apoptosis detection kit. (d) The quantitative analysis of western blot of Cit-histone H3 in different groups of neutrophils. Neutrophils were treated with LPS and co-cultured with different concentrations of CS nanozyme for 3 h (1.56, 3.13, 6.25 μg/mL). DPI was used to as the negative control. n = 3 independent experiments per group. The data were presented as the means ± s.d. One-way ANOVA with Tukey's post hoc test was used for comparisons among multiple groups (d). Source data were provided as a Source Data file.

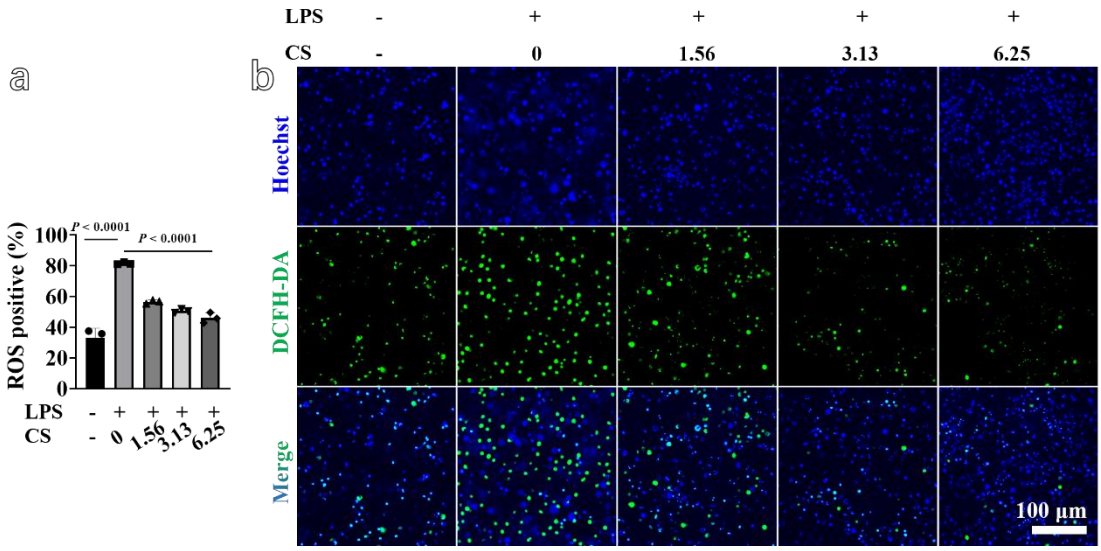

Figure S13. (a) Flow cytometric analysis and (b) confocal laser scanning microscopy (CLSM) images of the intracellular ROS in different groups of neutrophils. Neutrophils were treated with LPS, LPS co-cultured with CS nanozyme (1.56, 3.13, 6.25 μg/mL), LPS co-cultured with DPI for 3 h. n = 3 independent experiments per group. The data were presented as the means ± s.d. One-way ANOVA with Tukey's post hoc test was used for comparisons among multiple groups (a). Source data were provided as a Source Data file.

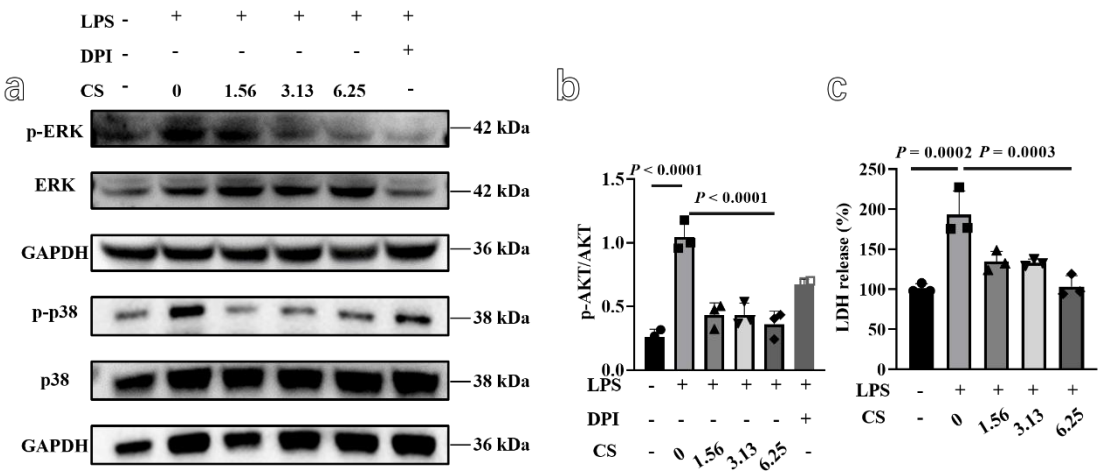

Figure S14. (a) Western blot analysis of p-ERK, ERK, p38, p-p38 in different groups of neutrophils. (b) The quantitative analysis of western blot of p-AKT/AKT in different groups of neutrophils. n = 3 independent experiments per group. (c) LDH release in different groups of neutrophils. Neutrophils were treated with LPS and co-cultured with different concentrations of CS nanozyme (1.56, 3.13, 6.25 μg/mL). DPI was used as the negative control. n = 3 independent experiments per group. The data were presented as the means ± s.d. One-way ANOVA with Tukey's post hoc test was used for comparisons among multiple groups (b and c). Source data were provided as a Source Data file.

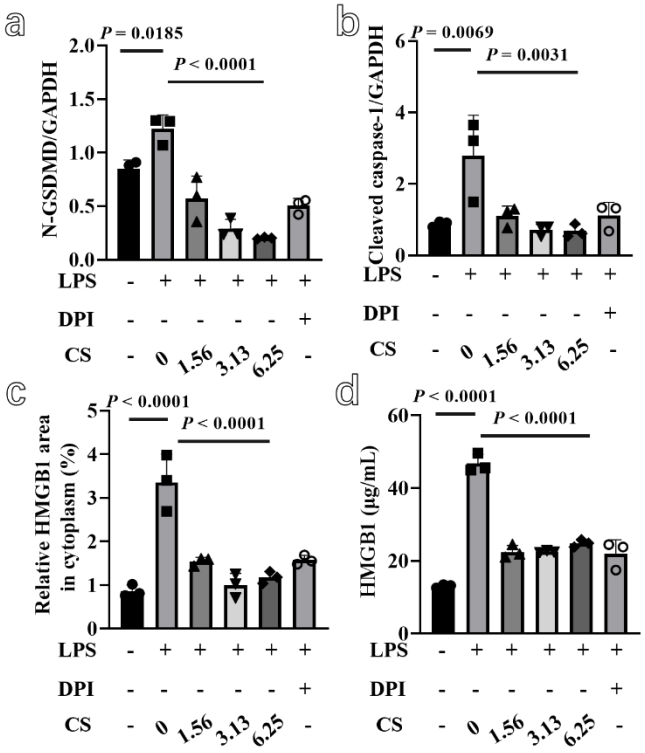

Figure S15. (a–b) The quantitative analysis of western blot of N-GSDMD/GAPDH and cleaved caspase-1/GAPDH in different groups of neutrophils. n = 3 independent experiments per group. (c) Quantitative analysis of the HMGB1 area in the cytoplasm by ImageJ. n = 3 independent experiments per group. (d) The HMGB1 released in the culture medium of neutrophils, assayed by ELISA. Neutrophils were treated with LPS and co-cultured with different concentrations of CS nanozyme for 3 h (1.56, 3.13, 6.25 μg/mL). DPI was used as the negative control. n = 3 independent experiments per group. The data were presented as the means ± s.d. One-way ANOVA with Tukey's post hoc test was used for comparisons among multiple groups (a, b, c, d). Source data were provided as a Source Data file.

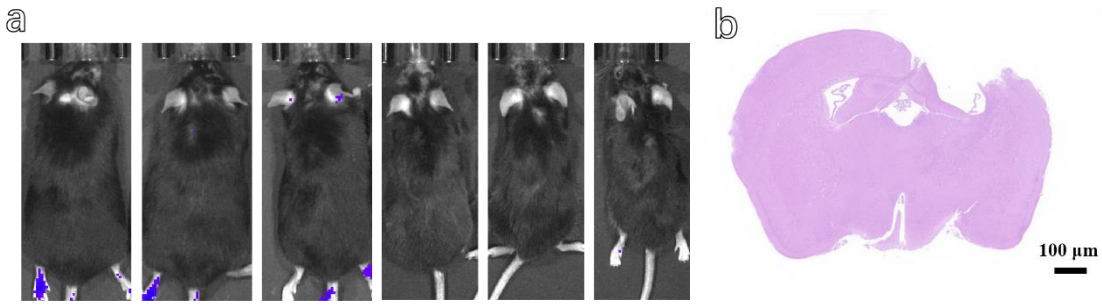

Figure S16. (a) Bioluminescence images of GL261-luciferase-bearing mice after treatment with surgery and CS nanozyme with DOX for 24 months. (b) H&E staining image of their brain slice.

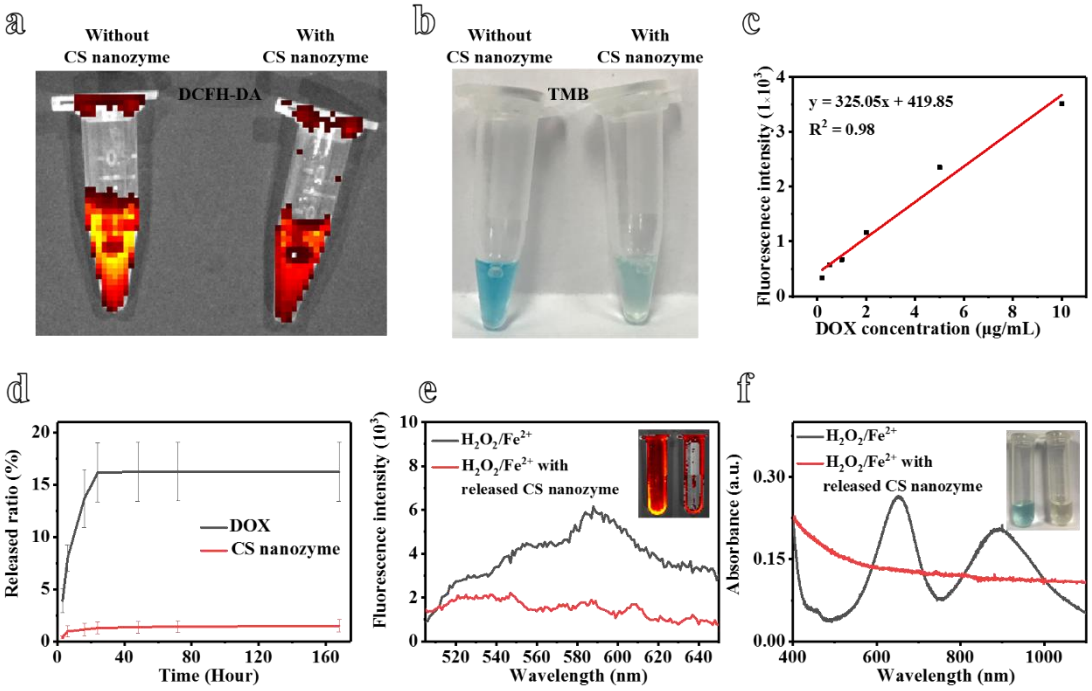

Figure S17. The ROS scavenging ability of CS nanozyme in hydrogel. (a) The DCFH-DA assay of ROS with or without CS nanozyme in hydrogel. (b) TMB assessment of ROS with or without CS nanozyme in hydrogel. (c) Concentration dependent fluorescence intensity of DOX at 593 nm. (d) The released ratio of CS nanozyme and DOX from hydrogel at different time points. (e) DCFH-DA assessment of ROS with or without CS nanozyme released from hydrogel (left insert: the fluorescence image of H_2O_2/Fe^{2+} solution without released CS nanozyme recorded by IVIS imaging system; right insert: the fluorescence image of H_2O_2/Fe^{2+} solution with released CS nanozyme). (f) TMB assessment of ROS with or without CS nanozyme released from hydrogel (left insert: the photograph of H_2O_2/Fe^{2+} solution without released CS nanozyme; right insert: the fluorescence image of H_2O_2/Fe^{2+} solution with released CS nanozyme). Source data were provided as a Source Data file.

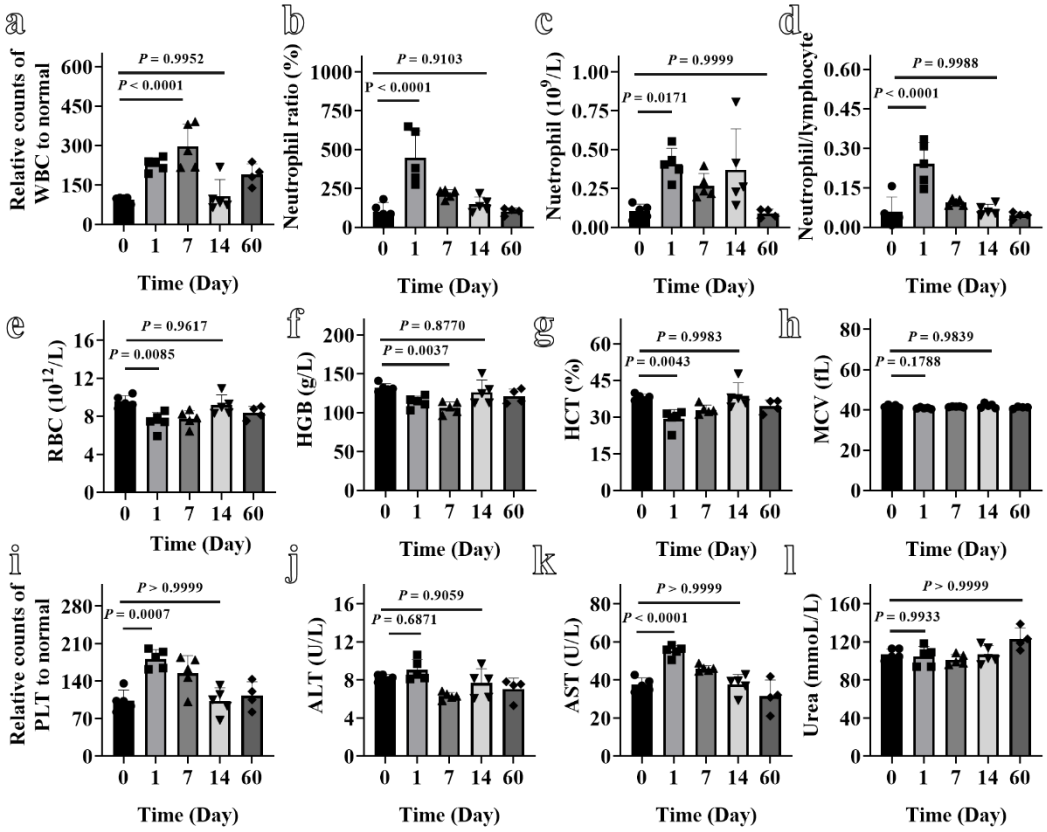

Figure S18. Time-dependent variation of blood indexes of GBM-bearing female C57BL/6J mice treated with CS nanozyme and DOX. (a) Relative counts of white blood cells (WBC) to normal. (b) Neutrophil ratio. (c) Neutrophil number. (d) Neutrophil/lymphocyte. (e) Red blood cell (RBC) counts. (f) Hemoglobin (HGB). (g) Hematocrit (HCT). (h) Mean corpuscular volume (MCV). (i) Relative counts of blood platelets (PLT) to normal. (j) Alanine aminotransferase (ALT). (k) Aspartate aminotransferase (AST). (l) Urea nitrogen (UREA). (n = 5 mice for all groups except the group of day 60, n = 4 mice). The data were presented as the means ± s.d. One-way ANOVA with Tukey's post hoc test was used for comparisons among multiple groups (a-l). Source data were provided as a Source Data file.

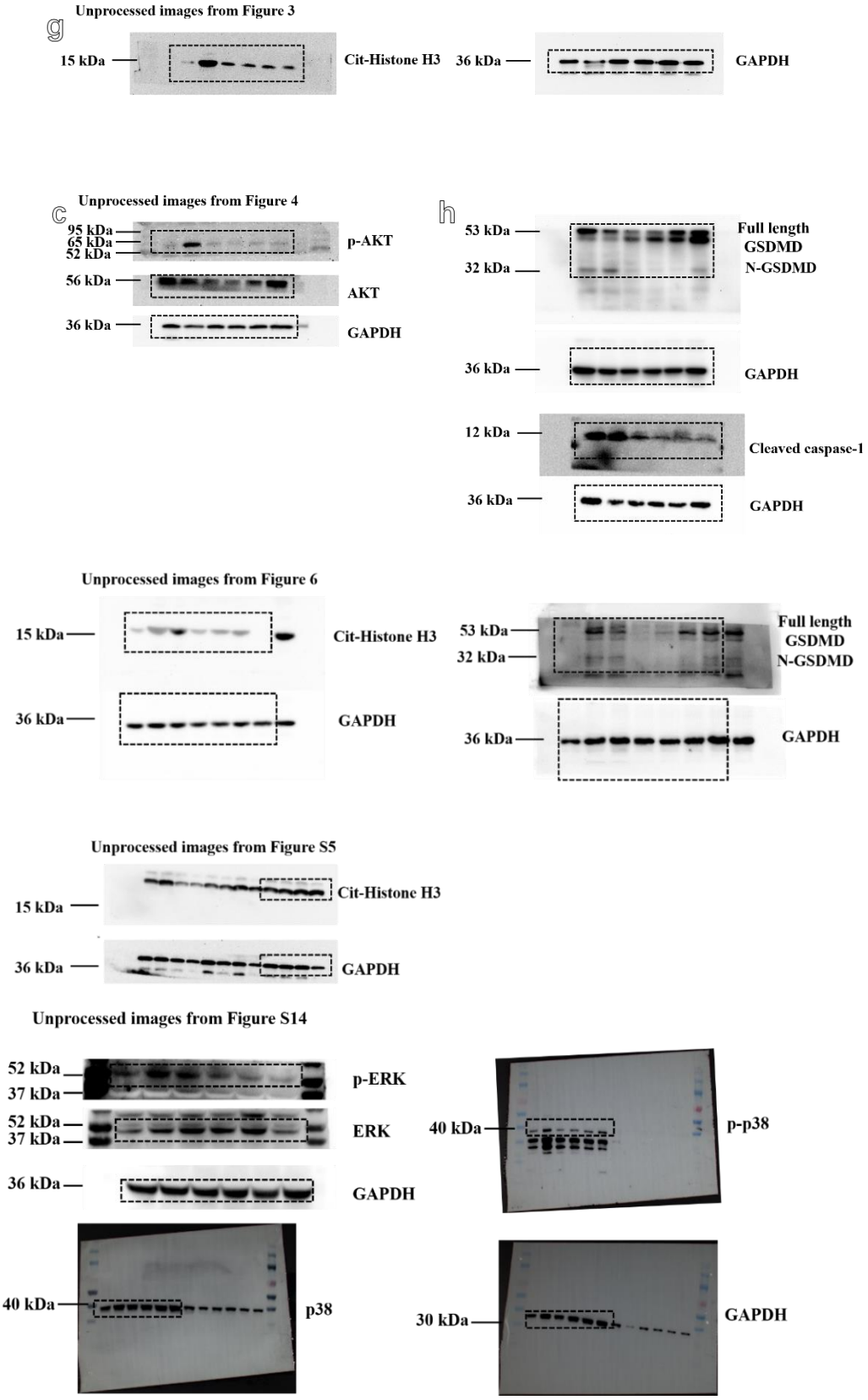

Figure S19. Unprocessed images for all western blots. Source data were provided as a Source Data file.